Reducing Cross-Track Geoid Gradient Errors around TOPEX/Poseidon and *Jason-1* Nominal Tracks: Application to Calculation of Sea Level Anomalies

J. DORANDEU, M. ABLAIN, AND P.-Y. LE TRAON

Space Oceanography Division, CLS, Ramonville–Saint-Agne, France

(Manuscript received 29 May 2002, in final form 15 May 2003)

ABSTRACT

A new technique is developed and tested to correct for cross-track geoid gradients in altimeter data. The proposed method is based on direct estimations of geoid variations around nominal tracks and on knowledge of ocean signal variability. Apart from measurement errors, ocean variability is demonstrated to be the major source of error in cross-track geoid estimations using altimeter measurements. The method thus uses the outputs of multimission ocean signal mapping procedures to improve the estimation of geoid features. A detailed error analysis shows that such a technique allows reduction of the estimation error by a factor of 2. Therefore, the method is applied taking advantage of the unprecedented TOPEX/Poseidon mission length. It provides a gain of 50%, in terms of sea level anomaly (SLA) variance reduction, in the cross-track geoid gradient correction used in collocating the repeat-cycle data. It also improves the estimation of altimetric mean profiles. From this study, local mean sea surface estimates can be inferred and applied to present and future altimetric missions, since they can be easily updated using more data. New altimetric missions like *Jason-1* and *Envisat,* with the same ground track as the former TOPEX/Poseidon and European Remote Sensing Satellite (ERS) missions, make the method even more relevant.

1. Introduction

The colinear analysis method has been used for many years in the field of altimetry to compute sea level anomalies (SLAs) relative to a reference mean profile (e.g., Cheney et al. 1983). The method obviously assumes a good orbit repetitiveness, since sea surface height (SSH) differences are computed from each cycle relative to a mean profile. This is a requirement for altimetric missions observing the sea level and ocean circulation. For instance, the Ocean Topography Experiment (TOPEX) Poseidon (T/P) ground track is maintained within a ± 1 km band at the equator.

In the colinear method, SSH estimations are interpolated and collocated at the reference profile locations. Along-track geoid signals, which represent the main contribution to SSH variations, are generally taken into account via the interpolation. On the contrary, if cross-track geoid variations are neglected when collocating the data onto the reference track, they translate into an error due to different sampled geoid signals from one repeat cycle to another. These errors have been shown to be as large as 10 cm rms in the vicinity of steep geoid features like seamounts and trenches (Brenner et al. 1990). In fact, only mean sea surface (MSS) slopes can be estimated from altimeter measurements, but at a few-kilometer scale, these slopes are dominated by geoid signals.

Brenner et al. (1990) demonstrated that the use of an MSS could be of great value when estimating geoid gradients. SSH values are locally referenced to MSS estimations to take account of geoid variations from one point to another. High-resolution and precise models are now available that have benefited from a long time series of precise altimetric measurements (e.g., Hernandez and Schaeffer, 2000; Wang 2001). Unfortunately, they poorly reproduce the shortest geoid wavelengths and thus remain unsatisfactory in regions of high geoid gradients.

This study presents a method for estimating geoid gradients around the T/P passes, directly based on the data themselves. Calculating the geoid gradients directly from the repeat-cycle data was first proposed and tested for *Geosat* data by Brenner et al. (1990). This is particularly important for the *Jason-1* mission, which will share the same ground track and will thus benefit from improved knowledge of local geoid gradients. In this article, we designate the T/P dataset as the first ground track from the T/P mission. Since August 2002, the T/P satellite ground track has been shifted so that the T/P and *Jason-1* ground tracks are interleaved.

The method presented herein takes advantage of the very long T/P time series. Substantial differences and improvements in the estimation method exist relative to

Corresponding author address: Dr. J. Dorandeu, CLS, 8–10 rue Hermès, Parc Technologique du Canal, 31526 Ramonville–Saint-Agne, France.
E-mail: dorandeu@cls.fr

the one described in Chambers and Tapley (1998), even if both studies locally adjust geoid variations around the nominal mean profile.

Particular attention is paid to error reduction using precise analyses of ocean variability. A complete method for removing ocean signals and other errors before geoid gradient adjustments is proposed and applied using 7 yr of T/P data. Knowledge of ocean variability is shown to be the key point in reducing estimation errors, together with the length of the altimetric time series. An error analysis is performed at global and local scales. The impact of the method is then investigated in deep geoid variation zones but is also considered in regions of high ocean variability.

A general description of the method is presented in section 2. The error-reduction scheme is discussed in section 3, wherein the ocean variability estimation is detailed and a precise error analysis is performed. Finally, in section 4, the method is applied to colinear calculations and compared to the method using a global MSS model. Improvements are quantified. An appendix showing how the method can be used to build a local MSS dedicated to one particular mission is then presented.

2. Method and general description of data

A nominal mean ground track is first built from 7 yr (1993–99) of T/P data as distributed by the Archiving, Validation and Interpretation of Satellite Oceanographic data agency (AVISO 1996), averaging the real data locations over the whole period. This mean track thus represents the most likely position of T/P data for this 7-yr period. It is sampled at the altimeter frequency, defining locations that can be used as reference points to compute cross-track geoid gradient estimations.

For the whole period, SSH values on individual passes are computed after data editing (Le Traon et al. 1994). SSH values are then sampled by an along-track interpolation using spline functions at locations defined as the orthogonal projections of the reference points onto the individual pass. For each reference location, SSH estimations from all available cycles at this location are obtained and can be plotted as a function of the cross-track distance from the mean profile. Figure 1 shows an example of such a SSH distribution in the north of the Tonga Islands, which is a region of deep geoid gradients. This distribution represents the typical signal that is intended to be estimated and analyzed in this study.

The method consists of fitting straight lines to these distributions to obtain an analytical expression of the cross-track geoid gradient for each reference location. Another method with simultaneous along-track and cross-track adjustments, using a local plane, can be found in Chambers and Tapley (1998). In fact, the two techniques are equivalent since in the present study an along-track interpolation has been performed prior to the cross-track adjustment.

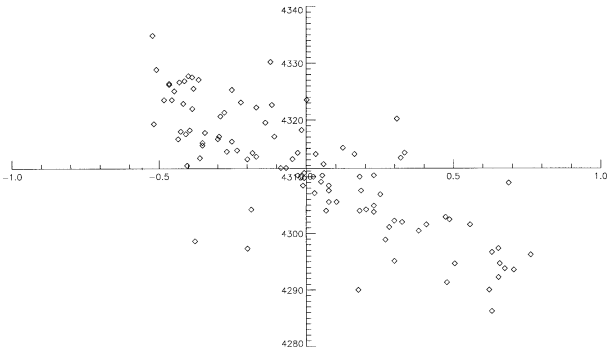

FIG. 1. SSH distribution (cm) in the area north of the Tonga Islands, for all available cycles over 3 yr of data at one reference track location, as a function of the cross-track distance (km) from the nominal pass.

Even though editing procedures have previously been applied, the estimation is obtained after two iterations to avoid contamination from remaining spurious data. A three-sigma criterion based on the first iteration is used before computing the final adjustment.

Finally, the method is very straightforward: it consists of adjusting a local slope at each reference location in the cross-track direction by least squares estimation; then SSH estimations are edited with a three-sigma criterion relative to this first adjustment; and then the final adjustment is performed from the selected measurements. The least squares procedure provides an estimation of the formal adjustment error. Both signal and error are analyzed in the following section.

3. Analysis of geoid signals and errors

a. Identification of major errors in the cross-track geoid gradient estimations

Error sources in the geoid gradient estimations come from ocean signals and errors. In fact, SSH signals can be split into static components, dynamic components, and noise: the steady part is represented by the geoid and the mean sea circulation, while the unsteady part is due to ocean variability, geophysical signals, and errors from both instrument measurement and geophysical corrections. Therefore, both ocean signals and errors impact the estimation of the static part, particularly the cross-track geoid gradient adjustment. Using longer time series should reduce the estimation errors. The unprecedented length of the T/P altimetric series should then allow us to compute precise geoid gradient estimations near the satellite track.

Cross-track geoid gradient estimations performed on T/P ascending passes using the method previously described are plotted in Fig. 2a. It clearly evidences high geoid gradient areas, like seamounts and trenches (i.e., north of the Tonga Islands, the Aleutian Islands), but also other regions of high ocean variability. For instance, higher signals are obtained in western boundary currents and their extensions, and in the equatorial zone.

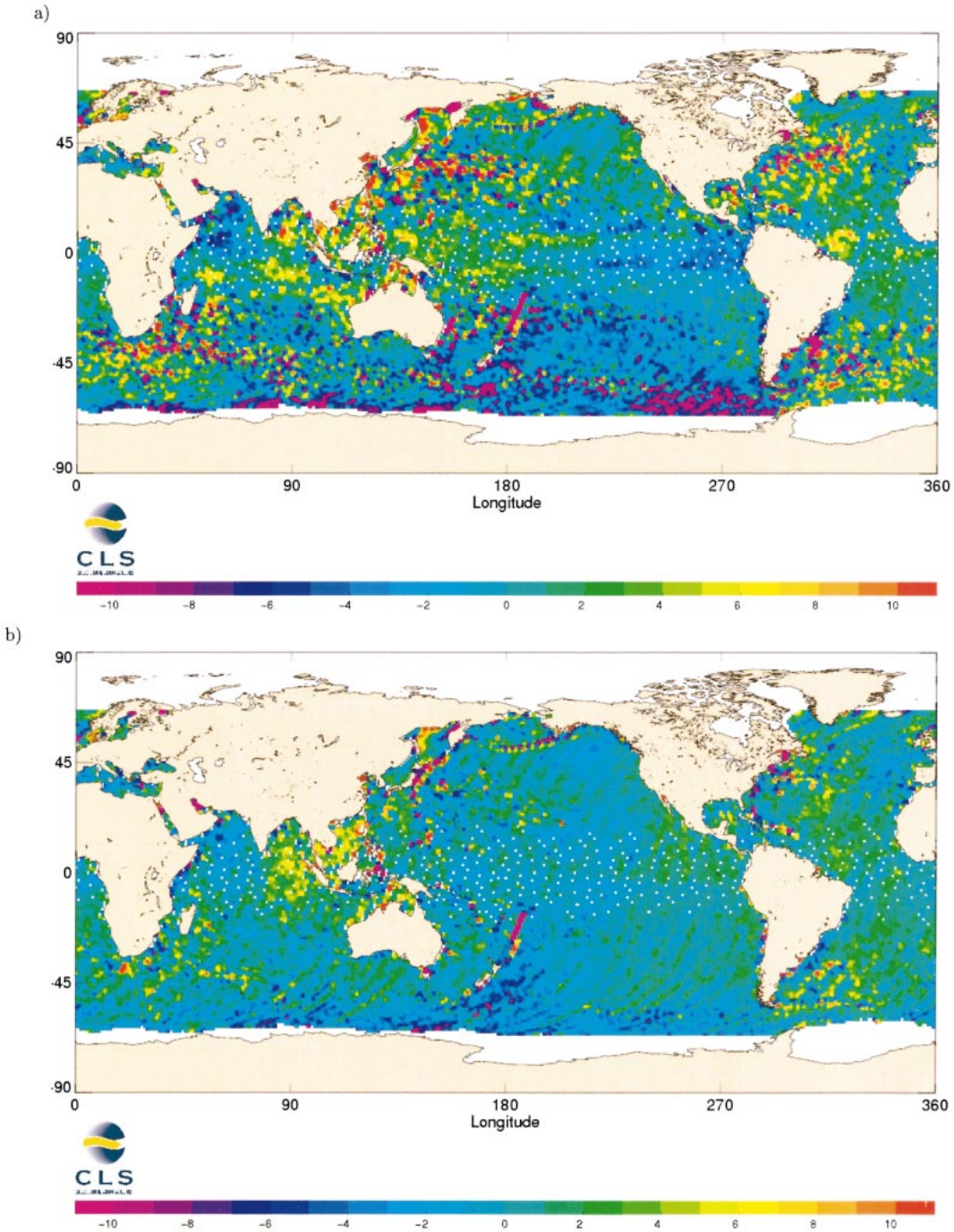

FIG. 2. Cross-track geoid gradient estimations (cm km^{-1}) from T/P ascending passes (a) without prior estimation and removal of ocean variability and (b) after ocean variability removal using MSLA maps.

This equatorial zone is particularly interesting because the adjusted signal seems very coherent and linked to the ocean variability. Ocean variability not only introduces noise in the adjustment but also biases the adjustment value itself. In fact, the distance between real and nominal tracks is not random but evolves slowly in time with periods on the order of months (Chambers and Tapley 1998). For example, the time sampling of an El Niño event in the equatorial zone by a continuous series of cycles could translate into an apparent cross-track slope because of the slow nonrandom displacement of the ground track from the nominal pass. This shows that ocean variability makes a big contribution to systematic and random errors in the cross-track geoid

gradient adjustments. Therefore, these signals must be properly removed prior to the adjustment.

b. Ocean variability estimation and reduction

In order to precisely estimate the ocean variability, SLA maps (MSLA) combining data from the T/P and *ERS-2* satellites have been used. These maps are routinely computed as AVISO products using an optimal analysis described in Le Traon et al. (1998) and Ducet et al. (2000). They provide SLA global estimations every 10 days, on a ¼° × ¼° grid. Prior to the optimal analysis, T/P and *ERS-2* SLAs are computed by repeat-track analysis. Therefore, one should suspect that cross-track geoid gradient errors also affect these maps. In fact, the impact of such errors on MSLA is totally negligible because these small-scale errors are filtered out in the mapping process.

An inverse method was recently developed to estimate long-wavelength errors due to residual orbit errors or high-frequency ocean signals poorly estimated by conventional geophysical corrections (Le Traon et al. 1998, Schaeffer et al. 2002, manuscript submitted to *J. Atmos. Oceanic Technol.*). These estimations are provided as along-track corrections for the whole TOPEX/Poseidon and ERS dataset. Long-wavelength signals represent a source of error in the geoid slope estimation. The impact of such signals should thus be tested.

In the geoid gradient estimation procedure, both ocean variability and long-wavelength errors are computed by linear interpolation at the time and location of altimeter measurements. Then they can be subtracted from SSH values before the adjustment.

c. Analysis of geoid slope signals

Figure 2b is similar to Fig. 2a, except that it is obtained after estimating and reducing the ocean variability using the procedure described above. Figures 2a and 2b show large differences, particularly in the equatorial zone and in high-ocean-variability areas. The impact of ocean variability on geoid gradient estimations is thus clearly evidenced. This justifies the use of a precise method for reducing the ocean variability before estimating geoid slopes from altimetric measurements.

To illustrate the impact of ocean variability, two portions of tracks were chosen. The first is an ascending track (track 223), which crosses the Tonga trench at around 20°S. Figure 3 shows three different cases: adjusting cross-track geoid slopes from 3 yr of T/P data without (bottom) and with (middle) SLA variability correction, and from 7 yr of data and SLA variability correction (top). Large differences, up to 10 cm km^{-1}, are observed between the cases with and without ocean variability reduction. These differences are large relative to the signal itself. Very significant discrepancies are observed in regions of high geoid gradient, around 20°S, but also in areas where the geoid gradient is very weak.

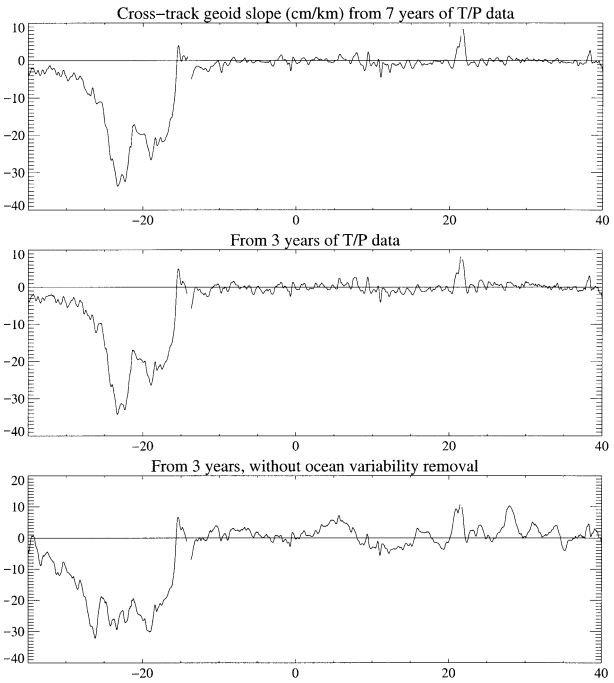

FIG. 3. Cross-track geoid gradient estimations (cm km^{-1}) along T/P track 223 (latitude in abscissa), for three different configurations: (top) from 7 yr of T/P data and after ocean variability reduction, (middle) from 3 yr of T/P data and after ocean variability reduction, and (bottom) from 3 yr of T/P data without ocean variability removal.

Thus, major errors due to ocean variability are likely to corrupt geoid slope estimations. On the contrary, the two cases with prior ocean variability reduction are very consistent. Only slight differences are noticed, due to the 3-yr estimation being noisier than the 7-yr estimation.

The second track crosses the Gulf Stream at around 40°N (pass number 115). This allows a better analysis of high-ocean-variability areas (Fig. 4). Nearly the same conclusions can be drawn. Large signals appear when no ocean variability reduction is performed, leading to differences larger than 15 cm km^{-1} relative to the other cases in the Gulf Stream region. In this high-variability area, the impact of the time series length is also more significant since differences of about 3 cm km^{-1} are observed between the estimations based on 3 and 7 yr.

In our method, estimations of cross-track geoid slopes have been performed at each reference profile location, with a sampling of about 7 km. In order to refine the signal characterization and the along-track estimation noise, it could be interesting to reduce the along-track sampling. We have thus tested whether oversampling the reference profile could improve geoid slope estimations. In fact, it led to unrealistic estimations, with along-track oscillations in the geoid slope estimations (not shown here). With higher along-track sampling than the nominal one, two different subsets of cycles are indeed alternatively used at each point of the reference profile. Since the slopes derived from the two different

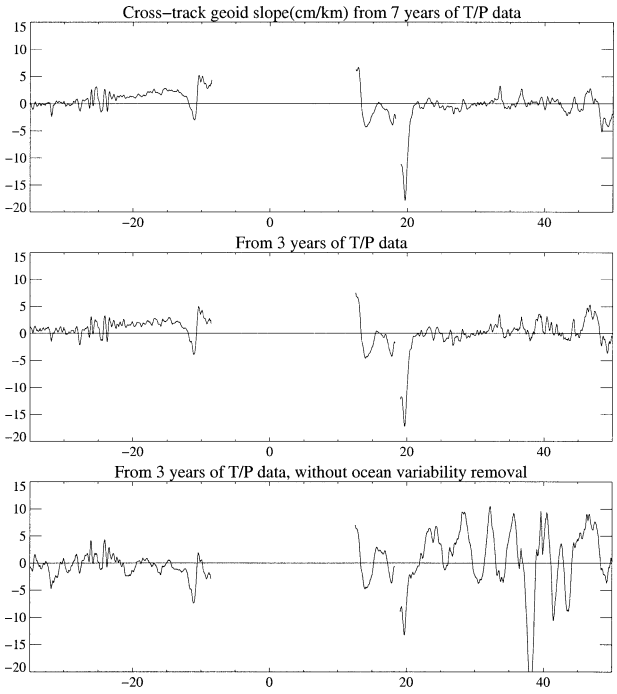

FIG. 4. Cross-track geoid gradient estimations (cm km^{-1}) along T/P track 115, which crosses the Gulf Stream at around 40°N (latitude in abscissa), for three different configurations: (top) from 7 yr of T/P data and after ocean variability reduction, (middle) from 3 yr of T/P data and after ocean variability reduction, and (bottom) from 3 yr of T/P data without ocean variability removal.

subsets are slightly biased, this leads to alternate variations along the reference track. Thus, geoid slope estimations are performed every 7 km along the reference track and estimations at other locations are computed using a cubic-spline along-track interpolation.

d. Error analysis

The different geoid slope estimation cases are also compared analyzing the formal adjustment error. The formal error is computed from the least squares method. This error does not represent the systematic error.

1) GLOBAL ANALYSIS

The error maps are shown on Fig. 5 in three different cases: the two first cases are obtained from 3 yr of T/P data without and with SLA variability correction, respectively. The last case is from 7 yr of T/P data after SLA variability correction. The comparison between the first two cases shows that with SLA variability removal the error estimates are reduced by a factor of at least 2. The adjustment error largely decreases in all ocean areas but more particularly in high-variability zones, such as western boundary currents and the equatorial zone. This demonstrates the importance of a precise SLA variability estimation method. Even with long altimetric time series, such a method is needed to reduce the major source of error prior to geoid signal adjustments. Removing only seasonal signals, for instance, can partly improve the results, but it is clearly not sufficient and even inadequate, given the complex spectrum of ocean variability.

The use of a longer time series obviously reduces the formal adjustment error. However, important adjustment errors, of about 2 cm km^{-1}, still remain in regions of high ocean variability. In these areas, the SLA variability is mainly due to mesoscale signals that can be only partially resolved in the mapping procedure. Semienclosed seas appear with higher error because of fewer SSH observations. Figure 5 also shows that the adjustment error pattern seems latitude dependent. In fact, at high latitudes, cross-track distances from the nominal profile decrease in average and explain why higher adjustment formal errors are obtained in these areas.

The influence of the time series length used in geoid signals adjustments is analyzed in Fig. 6. It presents the global error mean value for the whole of track 223, as a function of the time series length. The results show that the global estimation error consistently decreases with the length of the altimetric time series. With a 7-yr estimation, the global mean estimation error is about 0.8 cm km^{-1}, which represents an error reduction of about 50% relative to 2 yr of data. The figure also suggests that results could still be slightly improved by more data analysis. But, in fact, as shown in the figure, less than 5% error reduction can be expected from one more year of T/P data. The standard deviation of the adjustment error also decreases when increasing the amount of data used. This shows that the error becomes more uniform along this particular track, because adding more data particularly reduces the errors in areas of high ocean variability.

2) ANALYSIS OF SELECTED TRACKS

Track 223 is again used to precisely analyze the estimation errors in different configurations. The difference between the two upper blue curves in Fig. 7 is only due to SLA variability reduction before cross-track geoid slope estimation. The error decreases by a factor of at least 2 for the whole pass, but the error reduction is particularly significant in the Tonga trench region, around 20°S, where the formal adjustment error is divided by 3. After ocean variability reduction, the adjustment error is now much more homogeneous from one portion of the track to another. The lower red curve is obtained after ocean variability reduction, using 7 yr of data. Compared to the 3-yr estimation, the error has been uniformly reduced by about 40% and is about 1 cm km^{-1} in this case.

In addition to SLA variability reduction, the removal of long-wavelength signals estimated by an inverse method has been tested in the 3-yr case. This leads to an interesting adjustment error reduction of about 5%–10% and seems particularly significant at high latitudes, where high-frequency signals and long-wavelength er-

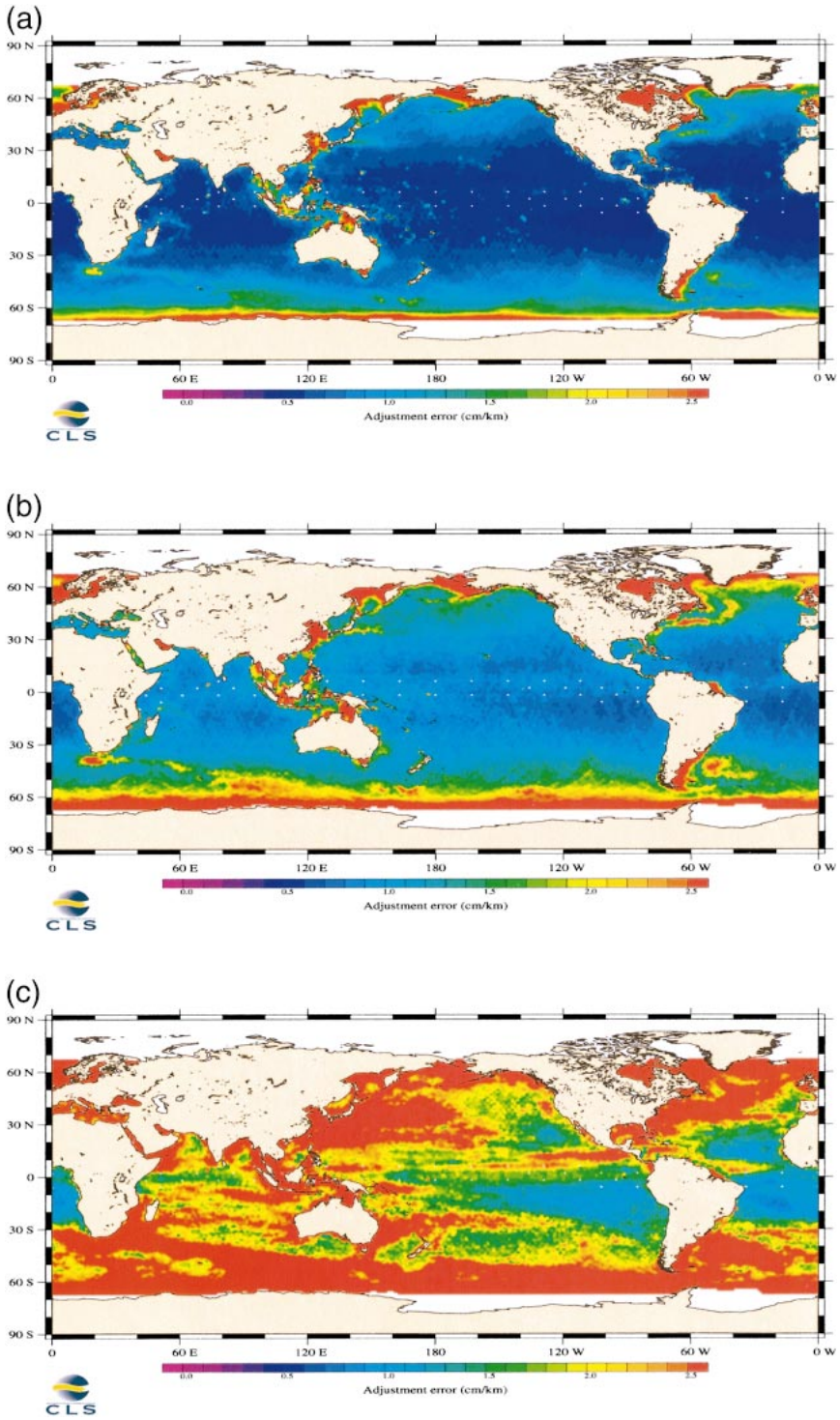

FIG. 5. Cross-track geoid gradient estimation error (cm km^{-1}), for three different configurations: (top) from 7 yr of T/P data and after ocean variability reduction, (middle) from 3 yr of T/P data and after ocean variability reduction, and (bottom) from 3 yr of T/P data without ocean variability removal. The estimation error scale ranges from 0 to 2.5 cm km^{-1}.

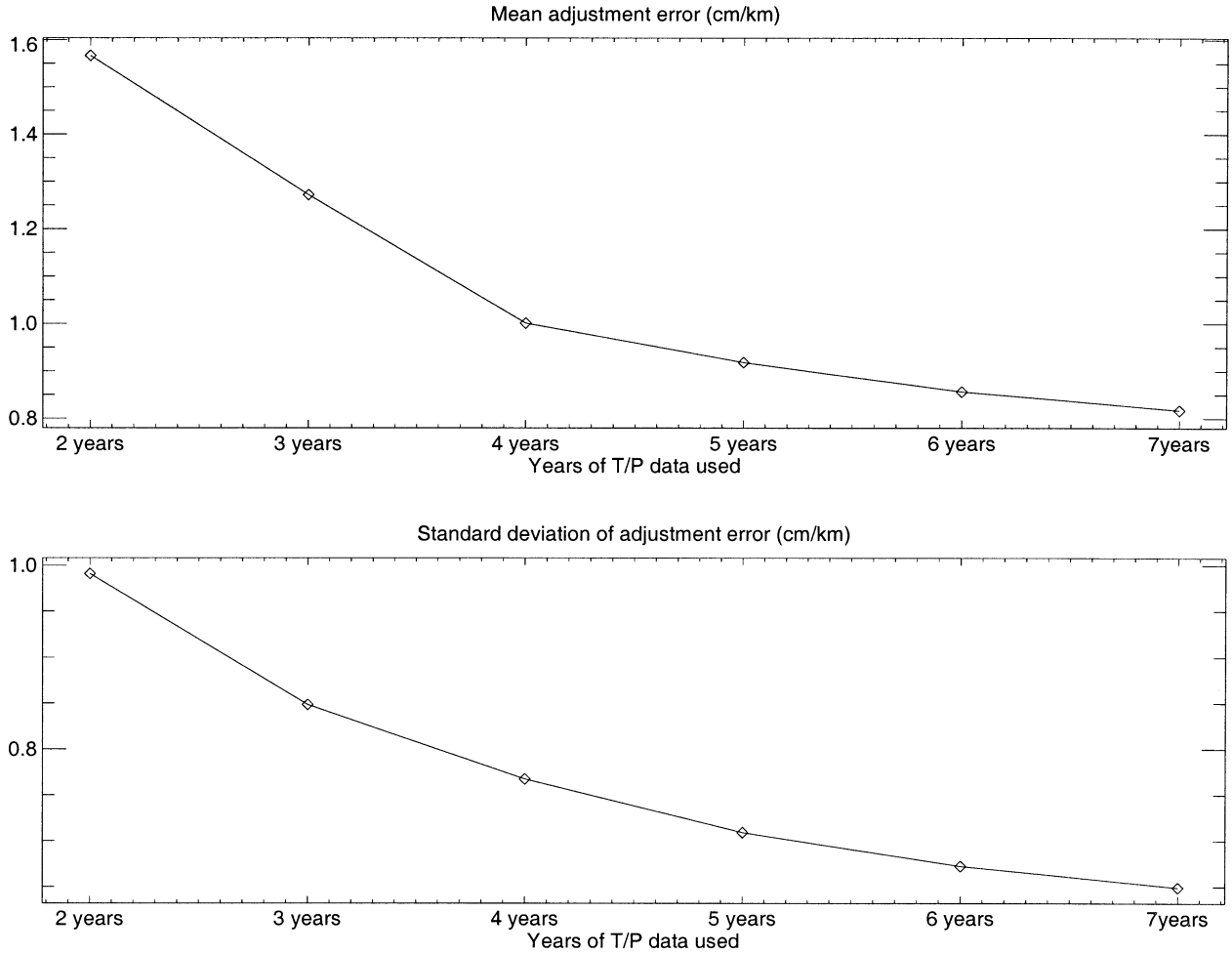

FIG. 6. (top) Mean and (bottom) std dev of the cross-track geoid slope adjustment formal error (cm km^{-1}) computed over the whole of pass 223, as a function of the amount (yr) of T/P data used in the adjustment.

rors are larger. Above 40°N, the error estimates for the 3-yr case are of the same order as for the 7-yr case without long-wavelength signal removal. Even if the gain in terms of adjustment error is weak compared to that achieved by ocean variability reduction, removing long-wavelength errors also improves the results in a nonnegligible manner.

Finally, the complete proposed method consists of removing both ocean variability estimations and long-wavelength signals before adjusting cross-track geoid slopes around the altimeter nominal path.

4. Impact of geoid slope corrections on SLA variability computed from colinear analysis

The previous estimations are used to correct for cross-track geoid errors while computing SLA from colinear analysis. During the interpolation at the reference mean track locations, geoid slopes are taken into account and used as an SSH correction. This section analyzes how this new correction reduces the SLA variability as estimated from repeat-track analysis when compared to no correction at all and to the correction derived from a global MSS model.

a. Global analysis

Figure 8a maps the gain in percentage of SLA variance achieved by using the cross-track geoid gradient correction. The global mean gain in variance is about 1% compared to the case with no correction, which corresponds to 1 cm^2 of variance. This is a low value, but the gain in variance can be considerably larger in regions of deep geoid features, like north of Tonga Islands, around the Aleutian Islands, in the northwest Pacific, and near the western coast of South America. In these zones, the gain in variance is much higher than 5%. However, in some equatorial zones, the SLA variance increases after correcting for the cross-track geoid slope. In these regions, waves propagating in the zonal direction generate high ocean variability. Correlation

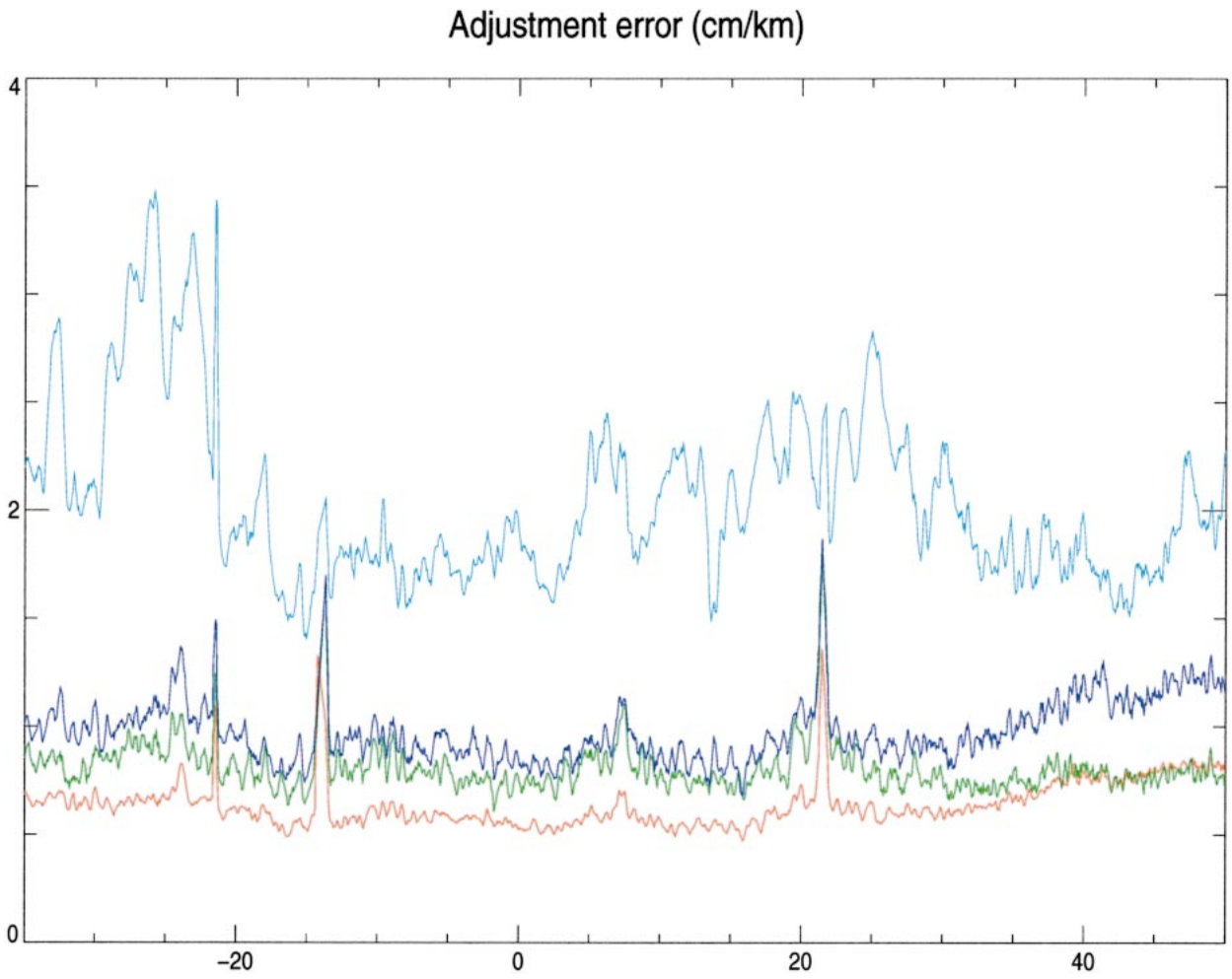

FIG. 7. Local analysis of cross-track geoid slope estimation error (cm km^{-1}) along pass 223 (latitude in abscissa): (light blue) geoid slope estimation error from 3 yr of T/P data, without ocean variability correction; (dark blue) geoid slope estimation error from 3 yr of T/P data, with ocean variability correction; (green) geoid slope estimation error from 7 yr of T/P data, with ocean variability correction; (red) geoid slope estimation error from 3 yr of T/P data, with ocean variability correction and long-wavelength signal removal.

between the ocean signals and the applied correction might explain the variance increase.

In order to assess the validity and quality of our geoid gradient estimation method, the CLS_SHOM98.2 MSS global model has been used to correct for the geoid gradient errors when computing colinear differences. The same kind of map can be produced in this case (Fig. 8b). The same general patterns are observed, particularly in the equatorial band. However, the gain in variance is weaker: Fig. 8b shows more red and fewer blue areas than Fig. 8a. The direct proposed geoid slope estimation method improves the correction by about 50% relative to the correction based on a global MSS, in terms of SLA variance reduction. Thus this validates the method. Indeed, even if this validation does not use an independent dataset, it is the case for the two methods: the method proposed here and the one derived from a global MSS. Note that these results were derived from the exact 3-yr period over which the reference mean profile used in the CLS_SHOM98.2 MSS was computed. On the contrary, geoid slopes have been estimated using the proposed method from 7 yr of data. These estimations are thus not exactly fitted on the geoid slopes sampled during the considered time period. And yet the method improves the results, showing the validity and reliability of the estimated geoid gradients.

ANALYSIS OF SELECTED TRACKS

The gain in repeat-track variance when using the new cross-track geoid gradients is analyzed on track 223 (Fig. 9). The geoid slope estimation error, the geoid slope signal, and the ocean variability as derived from the SLA maps are also plotted on the same figure. The gain in variance can be as large as 100 cm^2 in areas of strong geoid slopes. Apart from these zones, of course, the gain in variance is much weaker, as already shown in the previous section.

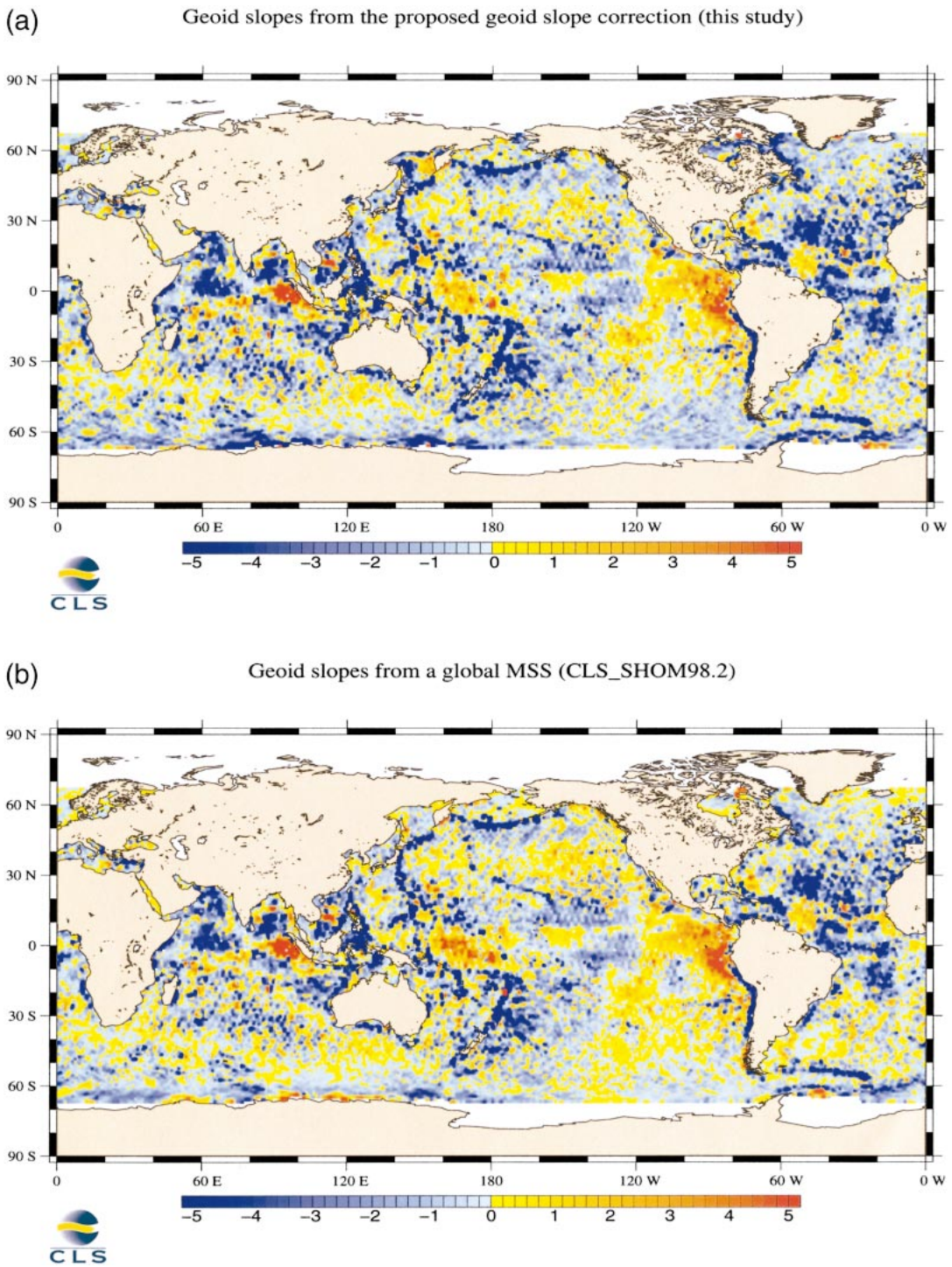

FIG. 8. Gain in percentage of T/P SLA variance when using a cross-track geoid slope correction from (a) the proposed method (this study) and (b) a global precise MSS (CLS_SHOM98.2). Units are in percentage of SLA variance. Negative values (blue bins) mean variance reduction relative to the case without geoid gradient correction. Positive values (red bins) mean variance increase.

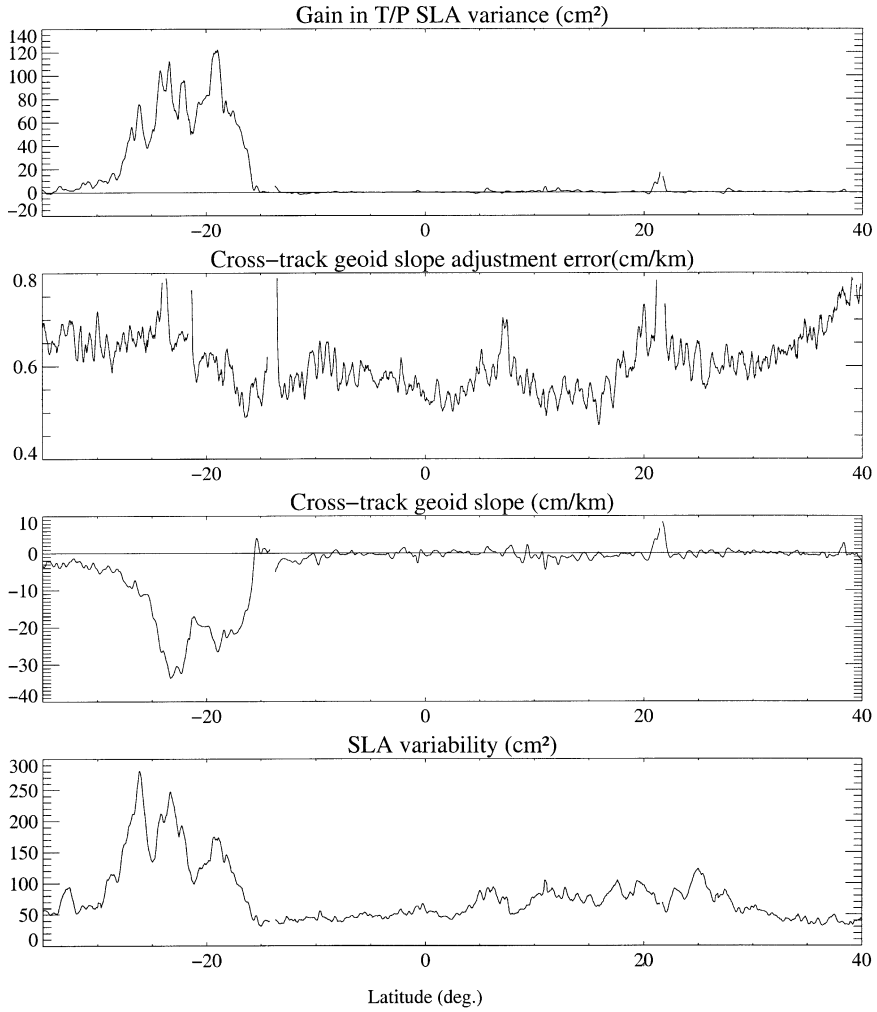

FIG. 9. Local analysis along T/P track 223. From top to bottom: gain in T/P SLA variance (cm^2) when using the proposed cross-track geoid slope correction, cross-track geoid slope estimation errors (cm km^{-1}), cross-track geoid slope estimations (cm km^{-1}), and variance of SLA variability (cm^2).

It is interesting to notice in this particular case that the high ocean variability between −30° and −15°S has been correctly removed before estimating the geoid slope. Indeed, in this zone the adjustment error is not significantly higher than anywhere else on the track. This example again underlines the importance of precisely estimating the ocean variability prior to geoid gradient adjustments, particularly in areas where both steep geoid gradients and high ocean variability are present.

The same portion of track is again used in Fig. 10 to compare the present estimation method to a global MSS. The gain in variance obtained with the former method relative to the latter is plotted for two different configurations, depending on the way local geoid slopes are computed: (a) with and (b) without ocean variability correction prior to the adjustment.

The higher gain in variance of colinear differences is obtained when the ocean variability is not corrected prior to the adjustment (Fig. 10b). In fact, real ocean signals have been taken into account during the adjustment in this case, since the least squares method tends to minimize the variance of the signal. This shows that direct adjustments could significantly impact the ocean signal estimation, while our study only aims at estimating static geoid features.

The other result was obtained after ocean variability reduction. In this case, the higher gain in variance relative to the use of a global MSS, up to 8 cm^2, is located in areas of strong geoid variations, showing the better accuracy of the proposed method in such areas.

b. Impact on mean profiles

The colinear method is also used to compute mean profiles over long time series collocating and averaging

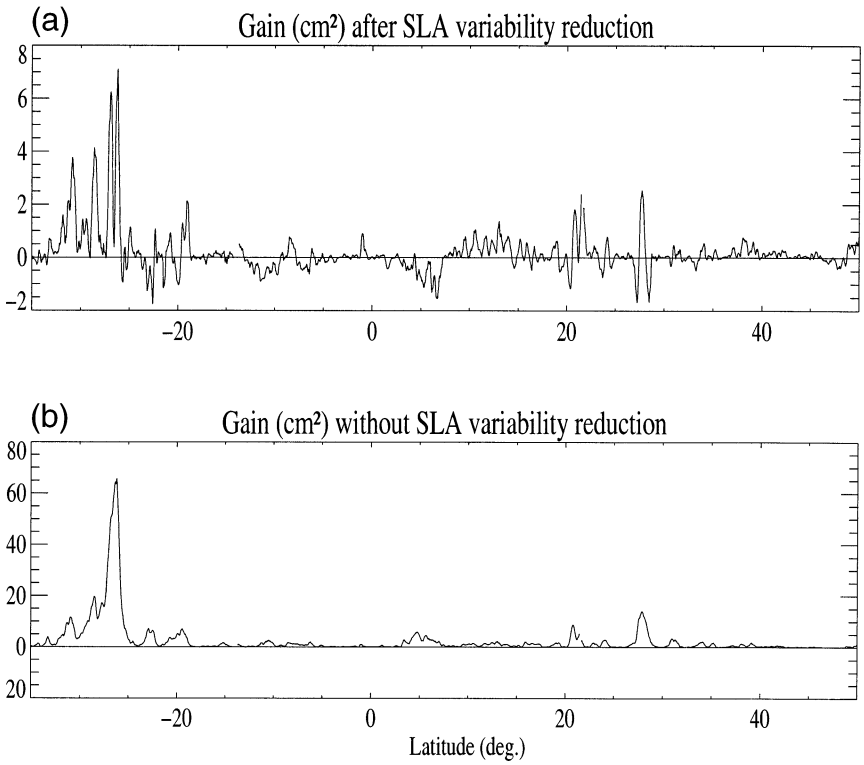

FIG. 10. Gain in SLA variance (cm^2) when using the proposed method rather than a global MSS to correct cross-track geoid errors in repeat-track analysis calculations when (a) SLA variability is corrected for prior to the adjustment and (b) adjustments are performed without ocean variability reduction.

SSH estimates at each reference track location. The mean SSHs are then used as a reference to compute SLA. While interpolating SSH values at the reference locations, cross-track geoid corrections are applied either from a global MSS (CLS_SHOM98.2 in this case) or from the proposed method. The intrinsic quality of both types of mean profiles is thus worth testing. To achieve this test, we computed the variance of the mean profile crossover differences, since it should be zero in an ideal case. The crossover variances are, respectively, 3.03 and 2.75 cm^2 for the mean profile computed using corrections from the global MSS and from the proposed method, a gain in variance of about 10%. Unlike the global MSS, in the present method the cross-track geoid slopes are estimated independently from one track to another. Although the method does not ascertain the consistency of geoid slopes at crossover points, it provides more precise estimations than a global MSS and improves the intrinsic quality of mean profiles.

5. Conclusions and perspectives

A direct method for estimating geoid slopes around the TOPEX/Poseidon ground track has been built and tested. It takes advantage of the long and precise TOPEX/Poseidon altimeter time series.

A great part of the study has focused on reducing estimation errors. Indeed, the error estimates should be provided, associated with geoid slope signal. This work emphasizes the importance of ocean variability estimation and removal prior to geoid slope adjustments. It shows that precise methods such as multimission optimal interpolation of ocean variability are needed in order to improve geoid feature determination without degrading the ocean signal itself. Applying these methods reduces the global geoid slope estimation error by a factor of about 2 and prevents ocean signal degradation. Despite the great precision of the T/P measurements, the study has also demonstrated the usefulness of long-wavelength error estimation and removal.

In addition, the error reduction implies the use of long altimeter time series. The study has shown that the stability of the global mean estimation error cannot be reached with time series shorter than 7 yr, that is, almost the whole TOPEX/Poseidon mission. So the continuity between the T/P and *Jason-1* missions on the same ground track will be of great interest when applying and improving this kind of method.

In terms of sea level anomaly (SLA) calculation, the method improves by about 50% the quality of the cross-track geoid corrections applied while computing the repeat-track differences, until now conventionally estimated using a global MSS. Given the good results provided by the method, the ± 1 km constraint around the

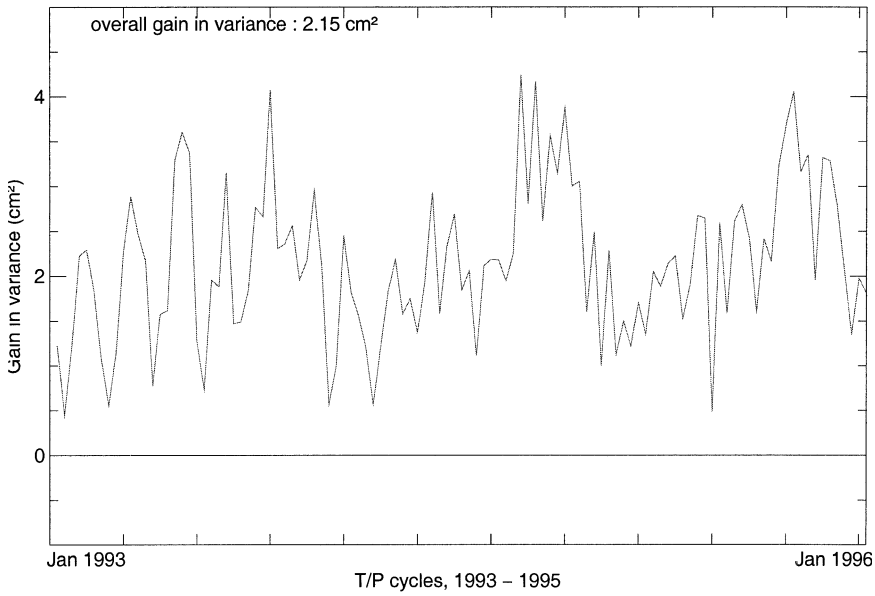

FIG. A1. Gain in T/P SLA variance when computed relative to the local along-track MSS derived from the proposed method rather than to the global MSS (CLS-SHOM98.2). The gain in SLA variance (cm^2) is computed for each T/P cycle over the 1993–95 period.

nominal track for altimetric missions could probably be relaxed, although there will be a slight degradation in terms of SLA calculation.

Better estimation of the local geoid slopes also improves the intrinsic quality of the mean profiles on the nominal track. This fact is particularly important with the *Jason-1* mission in mind, since *Jason-1* and TOPEX/Poseidon share the same nominal ground track.

From this work a complete algorithm can be proposed to build a ''local MSS.'' This algorithm is simply derived from the new mean profile and the geoid slope estimations. The quality assessment of this new local MSS and the way it can be implemented in an operational ground segment are presented in the appendix.

Acknowledgments. This study was supported by the French space agency CNES under Contracts SSALTO 2945-LOT 2-A3 and SALP 731/CNES/00/8435/00-CLS Lot-2.

APPENDIX

Using Geoid Slope Estimations to Build a Precise Local Mean Sea Surface

a. Method

Our calculation provides at each reference track location: the cross-track geoid gradient and the mean sea surface height (MSSH) computed after correcting for the cross-track geoid gradients, over a long time period (e.g., 7 yr of data). For any altimeter measurement point (A), one can perform the orthogonal projection (*P*) of this particular point onto the reference track, thus defining the distance (*d*) between A and the reference profile. Both MSSH and geoid slope can be interpolated at *P*. The local mean sea surface height (LMSSH) at the particular location can be computed as the MSSH at *P* corrected by the product of the slope at *P* and the cross-track distance *d*. This defines a straightforward algorithm that can be set up easily in any altimeter ground segment. It only needs as input auxiliary data the mean height and slope at the reference track locations.

As more data become available, upgrading this local mean sea surface would call for special processing involving precise ocean variability mapping. However, such mapping processes are already used routinely for near-real-time data and could thus be used in input for updating both mean height and slope of the reference profile.

b. Application to direct SLA calculation

The proposed method is applied along the T/P ground tracks to compute sea level anomalies (SLAs) relative to this local MSS. The SLA variance is computed cycle by cycle and compared to the results derived from the use of the CLS_SHOM98.2 global MSS over a 3-yr period (Fig. A1). For every T/P cycle, the SLA variance is reduced using the local MSS. Over the whole 3-yr period, the mean gain in variance is higher than 2 cm^2, that is, about 1.8%.

REFERENCES

AVISO, 1996: AVISO handbook for merged TOPEX/POSEIDON products. 3d ed. AVI-NT-02-101-CN, CNES, Toulouse, France, 201 pp.

Brenner, A. C., C. J. Koblinsky, and B. D. Beckley, 1990: A preliminary estimate of geoid-induced variations in repeat orbit satellite altimetric observations. *J. Geophys. Res.*, **95,** 3033–3040.

Chambers, D. P., and B. D. Tapley, 1998: Reduction of geoid gradient error in ocean variability from satellite altimetry. *Mar. Geod.*, **21,** 25–39.

Cheney, R. E., J. G. Marsh, and B. D. Beckley, 1983: Global mesoscale variability from collinear tracks of Seasat altimeter data. *J. Geophys. Res.*, **88,** 4343–4354.

Ducet, N., P.-Y. Le Traon, and G. Reverdin, 2000: Global high resolution mapping of ocean circulation from TOPEX/Poseidon and *ERS-1* and *-2*. *J. Geophys. Res.*, **105,** 19 477–19 498.

Hernandez, F., and P. Schaeffer, 2000: Altimetric mean sea surfaces and gravity anomaly maps inter-comparisons. AVI-NT-011-5242-CLS, CLS, Ramonville–Saint-Agne, 48 pp.

Le Traon, P.-Y., J. Stum, J. Dorandeu, P. Gaspar, and P. Vincent, 1994: Global statistical analysis of TOPEX and POSEIDON data. *J. Geophys. Res.*, **99,** 24 619–24 631.

——, F. Nadal, and N. Ducet, 1998: An improved mapping method of multisatellite altimeter data. *J. Atmos. Oceanic Technol.*, **15,** 522–534.

Wang, Y. M., 2001: GSFC00 mean sea surface, gravity anomaly, and vertical gravity gradient from satellite altimeter data. *J. Geophys. Res.*, **106,** 31 075–31 083.